Discotic Liquid Crystals of Transition Metal Complexes 37†: A Thermotropic Cubic Mesophase having $Pn\bar{3}m$ Symmetry of Phthalocyanine-based Derivatives

Masahiro Ichihara, Ayumi Suzuki, Kazuaki Hatsusaka and Kazuchika Ohta*

Smart Materials Science and Technology, Department of Bioscience and Textile Technology, Interdisciplinary Graduate School of Science and Technology, Shinshu University 386-8567 Ueda, Japan

Tel&FAX: 81-(0)268-21-5492, E-mail: ko52517@giptc.shinshu-u.ac.jp

Abstract

In order to obtain discotic compounds exhibiting a cubic mesophase, we synthesised two new series of discotic compounds, 2,3,9,10,16,17,23,24-octakis(4-alkoxyphenoxy)phthalocyaninato copper(II) (abbreviated as $(C_nOPhO)_8PcCu$: **1**, n = 10, 12, 14) and 2,3,9,10,16,17,23,24-octakis(3,4,5-trialkoxyphenoxy)phthalocyaninato copper(II) (abbreviated as $[(C_nO)_3PhO]_8PcCu$: **3**, n = 10, 12, 14) which consist of octakis(phenoxy)phthalocyaninato copper(II) as the same central core and eight and twenty-four long alkoxy chains in the periphery, respectively. Their mesomorphic properties of discotic compounds were compared together with those of the previously reported 2,3,9,10,16,17,23,24-octakis(3,4-dialkoxyphenoxy)phthalocyaninato copper(II)

(abbreviated as $[(C_nO)_2PhO]_8PcCu$: **2**, n = 10, 12, 14). The phase transition behaviour of these discotic compounds (**1** ~ **3**) varies very much with the number of peripheral chains. Eight-chains-substituted $(C_nOPhO)_8PcCu$ (**1**) exhibited only one hexagonal columnar (Col_h) mesophase but did not exhibit a cubic mesophase. Sixteen-chains-substituted $[(C_nO)_2PhO]_8PcCu$ (**2**) exhibited various columnar mesophases. Moreover, the $[(C_nO)_2PhO]_8PcCu$ (**2**) derivatives for n = 12 and 14 exhibited a cubic mesophase with $Pn\bar{3}m$ symmetry (Cub($Pn\bar{3}m$)) in a very narrow temperature region (*ca.* 5 ~ 8 ^oC) at high temperatures. On the other hand, twenty-four-chains-substituted $[(C_nO)_3PhO]_8PcCu$ (**3**) exhibited the Cub($Pn\bar{3}m$) phase in a much wider temperature region (*ca.* 90 ^oC). Thus, it was revealed that these discotic compounds tend to exhibit a cubic mesophase with increasing the number and length of peripheral chains. It should be emphasized that $[(C_nO)_2PhO]_8PcCu$ (**2**) (n = 12, 14) and $[(C_nO)_3PhO]_8PcCu$ (**3**) (n = 10, 12, 14) are the first discotic compounds exhibiting a thermotropic Cub($Pn\bar{3}m$) phase.

†: See Ref. [1].

1. Introduction

[Insert figure 1 about here]

Cubic mesophase is a fascinating mesophase because it has a three dimensional structure and a lot of unresolved problems. Cubic mesophases are categorized into two systems: thermotropic system and lyotropic system. Thermotropic cubic mesophases are shown by rod-like molecules,

dendrimers and polycatenars [2-16], whereas lyotropic cubic mesophases are shown by lipid-solvent system and so on [17-22]. Each of the compounds exhibiting both two kinds of cubic mesophases consists of two incompatible parts: an aliphatic chain and an aromatic core or a polar group and a nonpolar group. The micro-segregation of incompatible parts induces the formation of a cubic mesophase structure [2]. Cubic mesophase structures are categorized into two types as illustrated in figure 1. One type is bicontinuous cubic mesophases (figure 1a) which consist of bicontinuous network. Another type is discontinuous cubic mesophases (figure 1b) which consist of micells or spherical molecules. Structure and symmetry of the cubic mesophases depend to some extent on the molecular shape and system (= thermotropic system or lyotropic system). Rod-like molecules and polycatenars of thermotropic system tend to exhibit a bicontinuous cubic mesophase with $Im\bar{3}m$ or $Ia\bar{3}d$ symmetry. Dendrimers of thermotropic system tend to exhibit a discontinuous cubic mesophase with $Pm\bar{3}n$ symmetry. When the interface curvature between the incompatible parts is small in lyotropic system, bicontinuous cubic mesophases tend to be formed with $Pn\bar{3}m$, $Ia\bar{3}d$ or $Im\bar{3}m$ symmetry. On the other hand, when the interface curvature is big in lyotropic system, the aggregate changes into spherical shape and discontinuous cubic mesophases tend to be formed with $Pm\bar{3}n$, $Im\bar{3}m$ or $Fm\bar{3}m$ symmetry [3].

[Insert figure 2 about here]

Thus, the thermotropic cubic mesophases of rod-like molecules, polycatenars and dendrimers

have been well revealed for their symmetries [2-16]. Thus, the investigation of these thermotropic cubic mesophases has been greatly progressed. However, there have been only three investigations of discotic compounds exhibiting a cubic mesophase [23-25], and the symmetries of their cubic mesophases have never been identified. Figure 2 shows the molecular formula of one of the discotic compounds exhibiting a cubic mesophase. The 2,3,9,10,16,17,23,24-octakis(3,4-dialkoxyphenoxy)phthalocyaninato copper(II) (abbreviated as $[(C_nO)_2PhO]_8PcCu$: **2,** n = 10 ~ 14) derivatives exhibit very rich columnar mesophases, and the derivatives for n = 11 ~ 14 exhibit a cubic mesophase in a very narrow temperature region at high temperatures, as previously reported [24]. In this work, we synthesized two new series of discotic compounds, 2,3,9,10,16,17,23,24-octakis(4-alkoxyphenoxy)phthalocyaninato copper(II) (abbreviated as $(C_nOPhO)_8PcCu$: **1**, n = 10, 12, 14) and 2,3,9,10,16,17,23,24-octakis(3,4,5-trialkoxyphenoxy)phthalocyaninato copper(II) (abbreviated as $[(C_nO)_3PhO]_8PcCu$: **3**, n = 10, 12, 14) which consist of octakis(phenyoxy)phthalocyaninato copper(II) as the same central core and eight and twenty-four long alkoxy chains in the periphery, respectively. Their mesomorphic properties of these three series of discotic compounds **1** ~ **3** were investigated to reveal the influence of the number of peripheral chains on the appearance of a cubic mesophase and their symmetry. As the results, it was found and established that the derivatives **2** and **3** are the first discotic compounds exhibiting a cubic($Pn\bar{3}m$) phase.

We wish to report here the interesting cubic mesophase having $Pn\bar{3}m$ symmetry of these phthalocyanine-based derivatives, **2** and **3**.

2. Experiments

2.1. Synthesis

[Insert schemes 1 and 2 about here]

Schemes 1 and 2 show the synthetic routes of novel Pc derivatives of $(C_nOPhO)_8PcCu$ (**1**) and $[(C_nO)_3PhO]_8PcCu$ (**3**), respectively. The starting materials of *p*-hydroxybenzaldehydo (scheme 1) and 3,4,5-trihydroxybenzoic acid ethylester (scheme 2) were purchased from Tokyo Chemical Industry (Tokyo Kasei). In scheme 2, 3,4,5-trialkoxybenzoic acid ethylester (**7**) was synthesized by the method of Meier et al [26] and 3,4,5-trialkoxybenzaldehyde (**9**) was prepared by the method of Lin et al [27]. The detailed procedures of the representative $(C_{10}OPhO)_8PcCu$ (**2a**) and $[(C_{14}O)_3PhO]_8PcCu$ (**3c**) derivatives were described bellow.

*2.1.1. 4-Decyloxybenzaldehyde (**4a**)*

4-Hydroxybenzaldehyde (3.0 g, 25 mmol), 1-bromodecane (6.0 g, 27 mmol), dry-DMF (60 ml) and K_2CO_3 (22 g, 0.16 mol) were refluxed for 4 h under nitrogen atmosphere. The reaction mixture was extracted with diethylether and washed with water. The organic layer was dried over Na_2SO_4

and evaporated. The residue was purified by column chromatography (silica gel, $CHCl_3$, Rf = 0.48) to give 6.9 g of yellow oil. Yield = 96 %. IR (cm^{-1}) 2924, 2853, 2732, 1697, 1602, 1258.

*2.1.2. 4-Decyloxyphenol (**5a**)*

4-Decyloxybenzaldehyde (**4a**) (8.0 g, 30 mmol) was dissolved in a mixed solvent [$CHCl_3$ (30 ml) and MeOH (30 ml)], and then *conc.* H_2SO_4 (0.41 ml) and 30 %–H_2O_2 (21 g, 0.18 mol) were added into the mixture. The mixture was stirred at room temperature for 28 h. The reaction mixture was extracted with $CHCl_3$ and washed with water. The organic layer was dried over Na_2SO_4 and evaporated. The crude product was purified by column chromatography (silica gel, $CHCl_3$, Rf = 0.25) and recrystallization from petroleum ether (b.p. 30 ~ 60 °C) to give 4.0 g of white crystals. Yield = 64 %。 M.p. = 70.5–71.0 °C. IR (KBr, cm^{-1}) 3373, 2954, 2918, 2851, 1515, 1242.

*2.1.3. 4,5-Bis(4-decyloxyphenoxy)-1,2-dicyanobenzene (**6a**)*

4-Decyloxyphenol (**5a**) (1.2 g, 4.7 mmol), 4,5-dichlorophthalonitrile (0.31 g, 2.1 mmol) and N,N-dimethylacetoamide (18 ml) were stirred and heated under nitrogen atmosphere. When the temperature of the reaction mixture was reached to 90 °C, eight portions of K_2CO_3 (0.58 × 8 g, 4.2 mmol) were added to the mixture every 5 minutes, and then the reaction mixture was stirred at 90 °C for 30 minutes. The reaction mixture was extracted with $CHCl_3$ and washed with water. The organic

layer was dried over Na_2SO_4 and evaporated. The residue was purified by column chromatography (silica gel, $CHCl_3$, Rf = 0.75) and recrystallization from hexane to give 0.80 g of white crystals. Yield = 60 %. M.p. = 111 ^oC. IR (KBr, cm^{-1}) 2952, 2918, 2850 (CH_2-CH_3), 2228 (CN), 1500 (Ar), 1211 (C-O). ^1H NMR ($CDCl_3$: TMS) δ 0.87–0.90 (t, CH_3, 6H), 1.28–1.84 (m, CH_2, 32H), 3.96–3.99 (t, O-CH_2, 4H), 6.95–7.05 (m, Ar-H, 10H).

*2.1.4. 2,3,9,10,16,17,23,24-Octakis(4-decyloxyphenoxy)phthalocyaninato copper(II) (**1a**)*

4,5-Bis(4-decyloxyphenoxy)-1,2-dicyanobenzene (**6a**) (0.20 g, 0.32 mmol), $CuCl_2$ (0.016 g, 0.12 mmol), 1-hexanol (2 ml) and DBU (4 drops) were refluxed for 23 h. Excess MeOH was added to the reaction mixture to precipitate the target compound. The precipitate was collected by filtration and washed with ethanol. The crude product was purified by column chromatography (silica gel, $CHCl_3$, Rf = 0.15) and recrystallization from hexane two times to give 0.15 g of green solid. Yield = 73 %. M.p. & c.p.: See Table 3.

*2.1.5. 3,4,5-Tri(tetradecyloxy)benzoic acid ethyl ester (**7c**)*

3,4,5-Trihydroxybenzoic acid ethyl ester (3.0 g, 15 mmol), 1-bromotetradecane (16 g, 58 mmol), dry-DMF (47 ml) and K_2CO_3 (6.8 g, 49 mmol) were refluxed for 7 h. The mixture was extracted with Et_2O and washed with water. The organic layer was dried over Na_2SO_4 and evaporated. The

residue was purified by recrystallization from acetone to give 10 g of white crystals. Yield = 87 %. M.p. = 46–47 ^{o}C. IR (KBr, cm $^{-1}$) 2920, 2850, 1706, 1589, 1215, 763. ^{1}H NMR ($CDCl_3$: TMS) δ0.86–0.89 (t, CH_3, 9H), 1.26–1.39 (m, CH_2, 60H), 1.37 (t, CH_3,3H), 1.39 (m, γ-CH_2, 6H), 1.83-1.86 (m, β-CH_2, 6H), 3.99–4.02 (m, α-CH_2, 6H,), 4.34-4.35 (q, CH_2, 2H), 7.25 (s, Ar, 2H).

*2.1.6. 3,4,5-Tri(tetradecyloxy)benzylalcohol (**8c**)*

A solution of 3,4,5-tri(tetradecyloxy)benzoic acid ethyl ester (**7c**) in dry THF was added dropwise to dispersion solution of $LiAlH_4$ (0.64 g, 17 mmol) in dry THF (40 ml). The reaction mixture was stirred at room temperature for 1 h. The mixture was treated with NH_4Cl aq., filtered to remove precipitates and evaporated. The residue was extracted with Et_2O and washed with water. The organic layer was dried over Na_2SO_4 and evaporated. The crude product was purified by recrystallization from acetone to give 8.0 g of white crystals. Yield = 84 %. M.p. = 60 ^{o}C. IR (KBr, cm^{-1}) 3356, 2920, 2850, 1591. ^{1}H NMR ($CDCl_3$: TMS) δ0.86–0.89 (t, CH_3, 9H), 1.25–1.81 (m, CH_2, 72H), 3.97 (m, OCH_2, 6H), 4.59 (s, CH_2OH, 2H), 6.55 (s, Ar, 2H).

*2.1.7. 3,4,5-Tri(tetradecyloxy)benzaldehyde (**9c**)*

A solution of 3,4,5-tri(tetradecyloxy)benzylalcohol (**8c**) (0.90 g, 1.2 mmol) in CH_2Cl_2 (50 ml) was added to a solution of prydinium chlorochromate (4.5 g, 20 mmol) in CH_2Cl_2 (50 ml). The mixture

was stirred at room temperature for 2 h. The mixture was filtered to remove precipitate and poured into column chromatography (silica gel, CH_2Cl_2, Rf = 0.88). The further purification was performed by recrystallization from acetone to give 6.0 g of white crystals. Yield = 86 %. M.p. = 61 ^oC. IR (KBr, cm $^{-1}$) 2954, 2917, 2849, 1692, 1588, 716. ^1H NMR ($CDCl_3$: TMS) δ0.88 (t, CH_3, 9H), 1.26–1.86 (m, CH_2, 72H), 4.30 (m, OCH_2, 6H), 7.07 (s, Ar, 2H), 9.82 (s, CHO, 1H).

*2.1.8. 3,4,5-Tri(tetradecyloxy)phenol (**10c**)*

3,4,5-Tri(tetradecyloxy)benzaldehyde (6.0 g, 8.1 mmol) (**9c**) was dissolved in a mixed solvent [$CHCl_3$ (80 ml) and MeOH (40 ml)], and then *conc.* H_2SO_4 (0.032 ml) and 30 %–H_2O_2 (5.6 g, 15 mmol) were added to the mixture. The reaction mixture was stirred at room temperature for 48 h. The mixture was extracted with $CHCl_3$ and washed with water. The organic layer was dried over Na_2SO_4 and evaporated. The residue was purified by column chromatography (silica gel, $CHCl_3$, Rf = 0.33) and recrystallization from acetone to give 3.1 g of white crystals. Yield = 53 %. M.p. = 63 ^oC. IR (KBr, cm $^{-1}$) 3299, 2919, 2851, 1598, 722. ^1H NMR ($CDCl_3$: TMS) δ0.89–0.86 (t, CH_3, 9H), 1.25 (m, CH_2, 72H), 3.91 (m, OCH_2, 6H), 4.48 (s, OH, 1H), 6.04 (s, Ar-H, 2H).

*2.1.9. 4,5-Bis[3,4,5-tri(tetradecyloxy)phenoxy)-1,2-dicyanobenzene (**11c**)*

3,4,5-Tritetradecyloxyphenol (1.7 g, 2.3 mmol) (**10c**), dry N,N'-dimethylacetoamide (15 ml) and

K_2CO_3 (2.4 g, 17 mmol) were stirred at 50 ^oC for 30 minutes under nitrogen atmosphere. 4,5-Dichlorophthalonitrile (0.20 g, 1.0 mmol) was added to the mixture. The reaction mixture was stirred at 50 ^oC for further 45 minutes under nitrogen atmosphere. The mixture was extracted with $CHCl_3$ and washed with water. The organic layer was dried over Na_2SO_4 and evaporated. The crude product was purified by column chromatography (silica gel, $CHCl_3$, Rf = 0.98) and recrystallization from acetone to give 1.8 g of white crystals. Yield = 99 %. M.p. = 67 ^oC. IR (KBr, cm^{-1}) 2919, 2850, 2239, 1577, 1217, 724. ^1H NMR ($CDCl_3$: TMS) 0.86–0.88 (t, CH_3, 18H), 1.28–1.85 (m, CH_2, 144H), 3.86–4.07 (m, O-CH_2, 12H), 6.04, 6.26, 7.08, 7.84 (s, Ar-H, 6H).

2.1.9.10. 2,3,9,10,16,17,23,24-Octakis[3,4,5-tri(tetradecyloxy)phenoxy]phthalocyaninato copper (II) ***(3c)***

4,5-Bis[3,4,5-tri(tetradecyloxy)phenoxy]-1,2-dicyanobenzene (0.60 g, 0.38 mmol) (**11c**), $CuCl_2$ (0.015 g, 0.11 mmol), 1-hexanol (5 ml) and DBU (10 drops) were refluxed for 18 h. Excess MeOH was added to the reaction mixture to precipitate target compound. The precipitate was collected by filtration and washed with MeOH, EtOH and acetone, respectively. The crude product was purified by column chromatography (silica gel, $CHCl_3$, Rf = 1.00) and recrystallization from ethyl acetate to give 0.44 g of green solid. Yield = 68 %. M.p. & c.p.: See Table 3.

II-2 Measurements

[Insert tables 1 and 2 about here]

Table 1 shows elemental analysis data and MALDI-TOF mass spectral data of $(C_nOPhO)_8PcCu$ (**1**) and $[(C_nO)_3PhO]_8PcCu$ (**3**). The elemental analysis was performed by using a Perkin-Elmer elemental analyzer 2400. The MALDI-TOF mass spectral measurement was performed by using a PerSeptive Biosystems Voyager DE-Pro spectrometer. Each of the electronic absorption spectra of $(C_nOPhO)_8PcCu$ (**2**) and $[(C_nO)_3PhO]_8PcCu$ (**3**) was recorded by using a HITACHI U-4100 spectrophotometer and summarized in Table 2. Each of the phase transition behaviours of these compounds was identified with polarizing optical microscope (Nikon ECLIPSE E600 POL) equipped with a Mettler FP82HT hot stage and a Mettler FP-90 Central Processor, differential scanning calorimetric analysis (Simadzu DSC-50 and Perkin-Elmer Diamond DSC) and thermal gravimetric analysis (Rigaku Thermo plus TG8120). The identification of these mesophases was performed by using a wide angle X-ray diffractometer equipped with Cu-Kα radiation (Rigaku Rad) and a handmade hot stage equipped with a temperature controller [28].

3. Results and Discussion

3.1. Phase transition behaviour

[Insert table 3 about here]

The phase transition temperatures and enthalpy changes of $(C_nOPhO)_8PcCu$ (**1**) and $[(C_nO)_3PhO]_8PcCu$ (**3**) are listed in Table 3. For comparison, those of the previously reported $[(C_nO)_2PhO]_8PcCu$ (**2**: n = 10, 12, 14) derivatives [25] are also included in this table. As can be seen from this table, $(C_nOPhO)_8PcCu$ (**1**) exhibited not a cubic mesophase but only one hexagonal columnar (Col_h) mesophase in an extremely wide temperature region (*ca.* 200 °C). On the other hand, $[(C_nO)_2PhO]_8PcCu$ (**2**) exhibited rich kinds of columnar mesophases, and a cubic mesophase for n = 11 ~ 14 in a very narrow temperature region (*ca.* 5 ~ 8 °C) at high temperatures, as mentioned above. $[(C_nO)_3PhO]_8PcCu$ (**3**) exhibited a cubic mesophase in a much wider temperature region (*ca.* 90 °C). Thus, it was revealed that the present discotic compounds tend to exhibit a cubic mesophase in a wider temperature region with increasing the number and/or length of peripheral chains.

3.2. Polarizing optical microscopic observation

[Insert figure 3 about here]

Figure 3a shows the photomicrograph of $(C_{10}OPhO)_8PcCu$ (**1a**) at 256 °C. As can be seen from this photo, it shows a dendric texture with C_6 symmetry which is characteristic of a Col_h mesophase [29].From this texture, this mesophase is assigned as a Col_h mesophase.

Figure 3b shows the photomicrograph of $[(C_{10}O)_3PhO]_8PcCu$ (**3a**) at 50 °C. As can be seen from this photo, it shows a mosaic texture characteristic of a rectangular columnar (Col_r) mesophase [30].

Therefore, this mesophase is assigned as a Col_r mesophase. On further heating of this Col_r mesophase, it transformed into a completely optically isotropic paste having no fluidity. Figure 3c shows the photomicrograph of this phase. The phase could not be identified only from the photomicrograph, so that the phase was tentatively denoted as an unidentified Y phase here. Figure 3d shows the photomicrograph of $[(C_{10}O)_3PhO]_8PcCu$ (**3a**) at 160 °C. When the phase was observed between two glass plates, it was optically isotropic. When this phase was observed on a glass plate without a cover glass plate, it gave an optically isotropic round shape texture developed from the isotropic liquid, as shown in figure 3c. However, there has been no mesophase exhibiting such a texture, as far as we know. Hence, we could not identify this phase from the microscopic observations.

3.3. Temperature-dependent X-ray diffraction studies

[Insert table 4 and figure 4 about here]

In order to investigate these mesophase structures in detail, temperature-dependent X-ray diffraction (XRD) studies were performed. The XRD data of $(C_nOPhO)_8PcCu$ (**1**) and $[(C_nO)_3PhO]_8PcCu$ (**3**) were summarized in table 4. Figure 4 shows the XRD pattern of $(C_{10}OPhO)_8PcCu$ (**1a**) at 200 °C. It shows a halo around $\theta = 20°$ corresponding to molten alkoxy chains, and four sharp peaks in the small angle region. The spacing ratio of these sharp peaks in the

small angle region was 1 : 1/√3 : 1/2 : 1/√7. It was characteristic of a Col_h phase [31], so that this mesophase could be unambiguously identified as a Col_h phase. Each of the mesophases of the other $(C_nOPhO)_8PcCu$ (**1b**, **c**) homologues could be also identified as the Col_h phase.

[Insert figure 5 and table 5 about here]

Figure 5a shows the XRD pattern of $[(C_{10}O)_3PhO]_8PcCu$ (**3a**) at 65°C. It shows a halo corresponding to molten alkoxy chains in the wide angle region and six sharp peaks in the small angle region. The 1/d values of the sharp peaks in the small angle region were well fitted to a rectangular reciprocal lattice with P2m symmetry, so that the mesophase could be identified as a Col_r(P2m) mesophase [31]. Figure 5b shows the XRD pattern of the Y phase at 75 °C. As can be seen from this figure, it shows only three halos around $2\theta = 3^o$, 10^o and 20^o, which closely resembles that of the columnar nematic phase of Ref. 32. The present Y phase may be a columnar nematic (N_c) phase, because the Y phase exists between the Col_r(P2m) phase and a bicontinuous cubic mesophase consisted of the branched columns, as mentioned below. However, this phase did not show any natural texture, as mentioned above. Further investigation is necessary to identify this phase. At the present stage, it is tentatively denoted as an unidentified Y phase. Figure 5c shows the XRD pattern of **3a** at 155 °C. It shows five sharp peaks in the small angle region and a halo corresponding to molten alkoxy chains in the wide angle region. This XRD pattern in the small angle region showing these five sharp peaks was completely different from those of columnar mesophases. Generally, such

an XRD pattern showing several sharp peaks in a very narrow angle region at the small angles may be characteristic of a cubic mesophase. The spacing ratio of these peaks in the small angle region was $1/\sqrt{6} : 1/\sqrt{8} : 1/\sqrt{9} : 1/\sqrt{12} : 1/\sqrt{14}$. These peaks could be well assigned to Miller indices (2 1 1), (2 2 0), (2 2 1), (2 2 2) and (3 2 1), respectively, for a cubic lattice. Hence, this phase could be identified as a cubic mesophase. In table 5 are summarized the extinction rules for the space groups of bicontinuous cubic mesophases reported to date [33, 34]. The present cubic mesophase symmetry was identified from the extinction rules in this table. The Miller indices (1 1 1), (2 2 1) and (3 1 1) should be remarkable. The reflections corresponding to these three Miller indices can be observed only for $Pn\bar{3}m$ symmetry. As can be seen from figure 5c, the peak corresponding to Miller index (2 2 1) appears. Therefore, it could be concluded from the extinction rules that this cubic mesophase has a $Pn\bar{3}m$ symmetry. The number of molecules in a cubic cell was calculated from the equation as follows.

$$Z = \frac{\rho \times a^3 \times N_A}{Mw}$$

In this equation, Z = the number of molecules in a cubic cell, ρ = density of molecules, a = lattice constant of a cubic cell, N_A = Avogadro's constant and Mw = molecular weight. If the density ρ is assumed as 1.0 gcm^{-3}, the Z value of the cubic mesophase of **3a** at 155 ^oC can be calculated to be 89. Hence, the unite cell of this cubic mesophase consists of 89 molecules. Similarly concluded, each of the cubic mesophases of the other $[(C_nO)_3PhO]_8PcCu$ (**3b**, **c**) homologues also has the same $Pn\bar{3}m$

symmetry.

[Insert table 6 and figure 6 about here]

Hereupon, the cubic mesophase of the previously reported $[(C_nO)_2PhO]_8PcCu$ (**2**) derivatives [24] was reinvestigated, because the symmetry was not studied. Table 6 shows the XRD data of the cubic mesophase of $[(C_nO)_2PhO]_8PcCu$ (**2b**, **c**) derivatives. Figure 6 shows the XRD pattern of the cubic mesophase of $[(C_{12}O)_2PhO]_8PcCu$ (**2b**) at 192 ^oC. As can be seen from this figure, the XRD pattern closely resembles that of the Cub($Pn\bar{3}m$) of $[(C_{10}O)_3PhO]_8PcCu$ (**3a**) (See figure 5a). Although their reflections were indexed in our previous work [24], the indexation may be wrong judging from the resemblance to the present XRD pattern of $[(C_{10}O)_3PhO]_8PcCu$ (**3a**). Hence, we reinvestigated them here. As the result, these reflections could be correctly indexed to (2 1 1), (2 2 0), (2 2 1), (3 1 1) and (3 2 1), respectively. The reflections indexed to (2 2 1) and (3 1 1) are characteristic of the $Pn\bar{3}m$ symmetry (See table 5). Therefore, the cubic mesophase of $[(C_{12}O)_2PhO]_8PcCu$ (**2b**) could be identified as Cub($Pn\bar{3}m$). Similarly, the cubic mesophase of another $[(C_{14}O)_2PhO]_8PcCu$ (**2c**) derivative could be also identified as Cub($Pn\bar{3}m$).

[Insert figure 7 about here]

Figure 7a shows schematic models of the aggregate structures of rod-like molecules in some mesophases [15]. Cubic ($Ia\bar{3}d$) mesophase consists of three-dimensional skeletons (figure 7a i) and an infinite periodic bicontinuous minimal surface (IPMS) (figure 7a ii) located between the skeletons.

The skeleton and IPMS should be formed by two different components incompatible with each other. These two different components correspond to the peripheral chains and the central stripe-like cores in the case of thermotropic smectic mesophases. Up to date, two structural possibilities of IPMS have been reported that IPMS may be formed by the central cores (figure 7a iii) or the peripheral chains (figure 7a iv). Even in both of the cases, the rod-like molecules form a layered structure and the layered structure may undulate to exhibit a cubic phase. This mechanism can be easily accepted because rod-like molecules preferentially form a layered structure (= smectic phase) (See figure 7a v and vi). Figure 7b illustrates a possible mechanism for discotic molecules to form a cubic mesophase. At first, we thought similarly to the case of rod-like molecules that discotic molecules form a layered structure (figure 7b 2) and the layered structure may undulate (figure 7b 3) to exhibit a cubic mesophase. However, those columns are, in this case, completely surrounded by the peripheral chains as illustrated in figure 7b 3, so that the columns can form neither three-dimensional skeleton nor IPMS. Therefore, discotic molecules should have a mechanism different from the rod-like molecules to form a cubic mesophase. Generally, discotic molecules tend to form one-dimensional columns (figure 7b 4) because of the strong π - π interaction between the central cores. Hence, it can be thought that the cubic mesophase of discotic molecules may consist of the columns (figure 7b 5). In order to form a cubic mesophase with the columns, the columns should be branched and undulated to form three-dimensional skeletons (figure 7b 6) because the columns cannot form a

layered structure for IPMS. Therefore, it is suggested that, in the cubic phase of discotic molecules, the central cores form branched and undulated columns to develop the thee-dimensional skeleton and their peripheral chains form IPMS. This is almost the same mechanism that columnar mesophases consisted of rod-like compounds transform into cubic mesophases proposed by Donnio et al. [35] Moreover, the branched and undulated columnar structures may generate larger void among the columns, compared with general columnar mesomorphic structures. Only peripheral chains can fulfil the void, so that longer peripheral chains or numerous peripheral chains should be needed to form a cubic phase. This is consistent with the result that the longer-chain substituted-derivatives (n = 12 and 14) in the sixteen-chains-substituted $[(C_nO)_2PhO]_8PcCu$ (**2**: n = 10, 12, 14) homologues and all the twenty-four-chains-substituted derivatives of the $[(C_nO)_3PhO]_8PcCu$ (**3**) homologues exhibited a cubic phase.

4. Conclusion

In order to obtain discotic compounds exhibiting a cubic mesophase, two new series of discotic compounds, $(C_nOPhO)_8PcCu$ (**1**) and $[(C_nO)_3PhO]_8PcCu$ (**3**), have been synthesized for n = 10, 12, and 14. Their mesomorphic properties were compared with those of the previously reported $[(C_nO)_2PhO]_8PcCu$ (**2**) derivatives for n = 10, 12, and 14. The phase transition behaviour of these discotic compounds (**1** ~ **3**) varies very much with the number of peripheral chains. The

eight-chains-substituted derivatives $(C_nOPhO)_8PcCu$ (**1**) exhibited only one hexagonal columnar (Col_h) mesophase but did not exhibit a cubic mesophase. The sixteen-chains-substituted derivatives $[(C_nO)_2PhO]_8PcCu$ (**2**) exhibited rich kinds of columnar mesophases and a cubic mesophase with $Pn\bar{3}m$ symmetry (Cub($Pn\bar{3}m$)) for n = 12 and 14 in a narrow temperature region (*ca.* 5 ~ 8 ^oC) at high temperatures. The twenty-four-chains-substituted derivatives $[(C_nO)_3PhO]_8PcCu$ (**3**) exhibited the Cub($Pn\bar{3}m$) phase in a much wider temperature region (*ca.* 90 ^oC). Thus, it was revealed that these discotic compounds tend to exhibit a cubic mesophase with increasing the number and/or length of peripheral chains. It should be emphasized that $[(C_nO)_2PhO]_8PcCu$ (**2**) (n = 12, 14) and $[(C_nO)_3PhO]_8PcCu$ (**3**) (n = 10, 12, 14) are the first discotic compounds exhibiting a thermotropic Cub($Pn\bar{3}m$) phase.

This work was supported by a Grant–in–Aid for the 21st Century COE Program and a Grant–in–Aid for Science Research (18039013) in a Priority Area "Super–Hierarchical Structures" from the Ministry of Education, Culture, Sports, Science and Technology, Japan.

References

[1] Part 36: Ichihara, M., Miida, M., Mohr, B., and Ohta, K., 2006, *J. Porphyrins Phthalocyanines,* in press.

[2] Tschierske, C., 1998, *J. Mater. Chem*., **8**, 1485–1508.

[3] Tschierske, C., 2002, *Curr. Opin. Colloid Interface Sci.*, **7**, 69–80.

[4] Kutsumizu, S., 2002, *Curr. Opin. Solid State Mater. Sci.*, **6**, 537–543.

[5] Diele, S., 2002, *Curr. Opin. Colloid Interface Sci.*, **7**, 333–342.

[6] Borisch, K., Diele, S., Göring, P., Kresse, H., and Tschierske, C., 1998, *J. Mater. Chem*., **8**, 529–543.

[7] Donnio, B., and Bruce, D. W., 1998, *J. Mater. Chem*., **8**, 1993–1997.

[8] Seo, J. S., Yoo, Y. S., and Choi, M. G., 2001, *J. Mater. Chem*., **11**, 1332–1338.

[9] Tschierske, C., 2001, *J. Mater. Chem.*, **11**, 2647–2671.

[10] Fazio, D., Mongin, C., Donnio, B., Galerne, Y., Guillon, D., and Bruce, D. W., 2001, *J. Mater. Chem*., **11**, 2852–2863.

[11] Kutsumizu, S., Yamada, M., and Yano, S., 1994, *Liq. Cryst*., **16**, 1109–1113.

[12] Kutsumizu, S., Ichikawa, T., Nojima, S., and Yano, S., 2000, *J. Phys. Chem. B*, **104**, 10196–10205.

[13] Kutumizu, S., Morita, K., Ichikawa, T., Yano, S., Nojima, S., and Yamaguchi, T., 2002, *Liq. Cryst*., **29**, 1447–1458.

[14] Kutsumizu, S., Morita, K., Yano, S., and Nojima, S., 2002, *Liq. Cryst*., **29**, 1459–1468.

[15] Impéror–Clerc, M., 2005, *Curr. Opin. Colloid Interface Sci.*, **9**, 370–376.

[16] Ujiie, S., and Mori, A., 2005, *Mol. Cryst. Liq. Cryst*, **437**, 25–31.

[17] Kraineva, J., Nicolini, C., Thiyagarajan, P., Kondrashkina, E., and Winter, R., 2006, *Biochim. Biophys. Acta*., **1764**, 424–433.

[18] Wang, X., Takahashi, H., Hatta, I., and Quinn, P. J., 1999, *Biochim. Biophys. Acta*., **1418**, 335–343.

[19] Wang, X., and Quinn, P. J., 2002, *Biochim. Biophys. Acta*., **1564**, 66–72.

[20] Feng, Y., Yu, Z. W., and Quinn, P. J., 2003, *Chem. Phys. Lipids*, **126**, 141–148.

[21] Staudegger, E., Prenner, E. J., Kriechbaum, M., Degovics, G., Lewis, R. N. A. H., McElhaney, R. N., and Lohner, K., 2000, *Biochim. Biophys. Acta*., **1468**, 213–230.

[22] Jordanova. A., Laichev, Z., and Tenchov, B., 2003, *Eur. Biophys. J.*, **31**, 626–632.

[23] Kohne, B., Praefcke, K., and Billard, J., 1986, *Z. Naturfrsch*, **41b**, 1036–1044.

[24] Billard, J., Zimmermann, H., Poupko, P., and Luz, Z., 1989, *J. Phys. France*, **50**, 539–547.

[25] Hatsusaka, K., Ohta, K., Yamamoto, I., and Shirai, H., 2001, *J. Mater. Chem*., **11**, 423–433.

[26] Meier, H., Proß, E., Zerban, G., and Kosteyn, F., 1988, *Z. Naturforsch*., **436**, 889–896.

[27] Lin, Y. C., Lai, C. K., Chang, Y. C., and Liu, K. T., 2002, *Liq. Cryst*., **29**, 237–242.

[28] Hasebe, H., 1991, Master Thesis, Shinshu University, Ueda, Japan, ch. 5; Ema, H., 1988, Master Thesis, Shinshu University, Ueda, Japan, ch. 7.

[29] Baehr, C., Ebert, M., Frick, G., and Wendorff, J. H., 1990, *Liq. Cryst.,* **7**, 601–606.

[30] Gray, G. W., and Goodby, J. W., 1984, *SMECTIC LIQUID CRYSTALS Textures and Structure*, (Philadelphia, Heyden & Son).

[31] Ohta, K., 2001, *Ekisho*, **6**, 61–71.

[32] Bock, H., Babeau, A., Seguy, I., Jolinat, P. and Destruel, P., 2002, *Chem. Phys. Chem.*, **6**, 532–535.

[33] Mariani, P., Luzzati, V., and Delacroix, H., 1988, *J. Mol. Biol.*, **204**, 165–189.

[34] Seddon, J. M., Robins, J., Gulik-Krzywicki, T., and Delacroix, H., 2000, *Phys. Chem.Chem. Phys*., **2**, 4485–4493.

[35] Donnio, B., Heinrich, B., Gulik-Krzywicki, T., Delacroix, H., Guillon, D., and Bruce, D. W., 1997, *Chem. Mater.*, **9**, 2951-2965.

Figure caption

Figure 1. Skeletones of infinite periodic bicontinuous minimal surface (IPMS) of bicontinuous cubic mesophases and schematic representation of discontinuous cubic pahses.

Figure 2. Molecular formula of $(C_nOPhO)_8PcCu$: **1** $[(C_nO)_2PhO]_8PcCu$: **2** and $[(C_nO)_3PhO]_8PcCu$: **3**.

Figure 3. Photomicrographs of $(C_{10}OPhO)_8PcCu$: **1a** and $[(C_{10}O)_3PhO]_8PcCu$: **3a**. (a): $(C_{10}OPhO)_8PcCu$: **1a** at 256 ^oC. (b): $[(C_{10}O)_3PhO]_8PcCu$: **3a** at 50 ^oC. (c): $[(C_{10}O)_3PhO]_8PcCu$: **3a** at 75 ^oC. (d): $[(C_{10}O)_3PhO]_8PcCu$: **3a** at 160 ^oC.

Figure 4. XRD pattern of $(C_{10}OPhO)_8PcCu$: **1a** at 200 ^oC.

Figure 5. XRD patterns of $[(C_{10}O)_3PhO]_8PcCu$: **3a** at various temperatures.

Figure 6. XRD pattern of [(C12O)2PhO]8PcCu: **2b** at 192 ^oC.

Figure 7. Possible formation mechanism of cubic mesophases. (a) For rod-like molecules: (i)

bicontinuous skeletons of cubic($Ia\bar{3}d$), (ii) an IPMS of cubic($Ia\bar{3}d$), (iii) an IPMS consisted of cores, (iv) an IPMS consisted of alkyl chains, (v) a smectic phase structure, (vi) molecular aggregation in the layer structure. (b) For discotic molecules: (1) a shape of discotic molecule, (2) a layer structure of discotic molecules (3) an undulated layer structure of discotic molecules (4) a columnar phase structure (5) bicontinuous skeletons of cubic($Pn\bar{3}m$), (6) a branched and undulated column of discotic molecules.

Scheme 1. Synthetic route of $(C_nOPhO)_8PcCu$: **1**. DMF = N,N'-dimethylformamide, DMAA = N,N-dimethylacetamide and DBU = 1,8-diazabicyclo[5,4,0]-7-undecene.

Scheme 2. Synthetic route of $[(C_nO)_3PhO]_8PcCu$: **3**. DMF = N,N'-dimethylformamide, PCC = pyridinium chlorochromate, DMAA = N,N-dimethylacetamide and DBU = 1,8-diazabicyclo[5,4,0]-7-undecene.

(a) Bicontinuous cubic phases

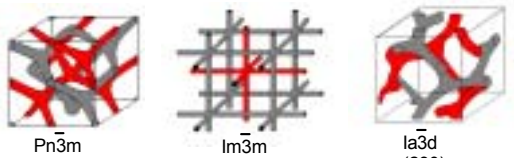

$Pn\bar{3}m$ (224) $Im\bar{3}m$ (229) $Ia\bar{3}d$ (230)

(b) Discontinuous cubic phases

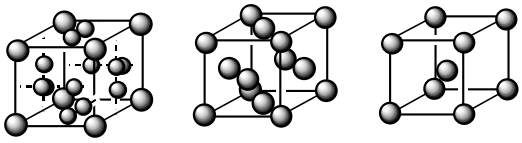

$Pm\bar{3}n$ (223) $Fm\bar{3}m$ (225) $Im\bar{3}m$ (229)

Figure 1.

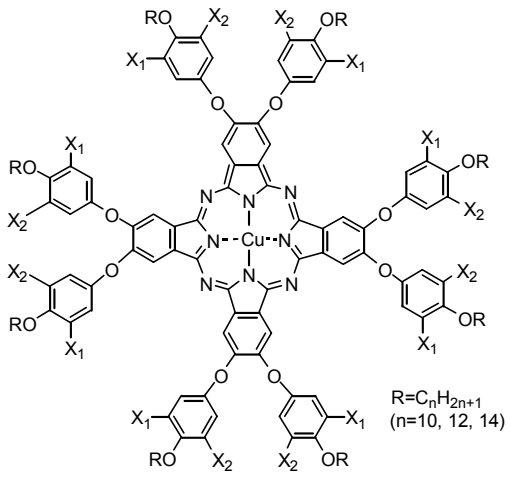

1: $(C_nOPhO)_8PcCu$; X_1 = H, X_2 = H
2: $[(C_nO)_2PhO]_8PcCu$; X_1 = OR, X_2 = H
3: $[(C_nO)_3PhO]_8PcCu$; X_1 = OR, X_2 = OR

Figure 2.

Table 1. MALDI-TOF mass spectral data and elemental analysis data of $(C_nOPhO)_8PcCu$: **1** (n=10, 12 and 14) and $[(C_nO)_3PhO]_8PcCu$: **3** (n=10, 12 and 14).

Compound	Mol. formula (Mol. wt)	Mass observed	Elemental analysis: Found (Calcd)/ %		
			N	C	H
1a: $(C_{10}OPhO)_8PcCu$	$C_{160}H_{208}N_8O_{16}Cu$ (2563.00)	2563.41	4.23 (4.37)	75.00 (74.98)	8.52 (8.18)
1b: $(C_{12}OPhO)_8PcCu$	$C_{176}H_{240}N_8O_{16}Cu$ (2787.43)	2786.13	3.84 (4.02)	76.05 (75.84)	9.04 (9.18)
1c: $(C_{14}OPhO)_8PcCu$	$C_{192}H_{272}N_8O_{16}Cu$ (3011.86)	3011.84	3.65 (3.72)	76.72 (76.57)	9.44 (9.10)
3a: $[(C_{10}O)_3PhO]_8PcCu$	$C_{320}H_{528}N_8O_{32}Cu$ (5063.20)	5059.78	2.25 (2.21)	76.25 (75.91)	10.61 (10.51)
3b: $[(C_{12}O)_3PhO]_8PcCu$	$C_{368}H_{624}N_8O_{32}Cu$ (5736.47)	5734.04	2.04 (1.95)	76.86 (77.05)	11.15 (10.96)
3c: $[(C_{14}O)_3PhO]_8PcCu$	$C_{416}H_{720}N_8O_{32}Cu$ (6409.75)	6407.53	1.75 (1.85)	77.95 (78.22)	11.32 (11.68)

Table 2. Electronic spectral data of $(C_nOPhO)_8PcCu$: **1** (n=10, 12 and 14) and $[(C_nO)_3PhO]_8PcCu$: **3**

Compound	Concentration[a] / $\times 10^{-6}$ mol l^{-1}	λmax/ nm (logε)				
		Soret-band		Q-band		
1a: $(C_{10}OPhO)_8PcCu$	6.81	290.0 (4.89)	338.0 (4.92)	616.0 (4.67)	654.0 (sh)	682.0 (5.41)
1b: $(C_{12}OPhO)_8PcCu$	6.69	290.0 (4.86)	340.0 (4.88)	616.0 (4.63)	654.0 (sh)	682.0 (5.36)
1c: $(C_{14}OPhO)_8PcCu$	5.95	290.0 (4.87)	338.0 (4.88)	616.0 (4.60)	654.0 (sh)	682.0 (5.34)
3a: $[(C_{10}O)_3PhO]_8PcCu$	6.62	291.0 (4.83)	340.0 (4.96)	615.0 (4.69)	652.0 (4.66)	684.0 (5.45)
3b: $[(C_{12}O)_3PhO]_8PcCu$	6.39	291.0 (4.83)	339.5 (4.96)	615.0 (4.68)	652.0 (4.65)	683.5 (5.43)
3c: $[(C_{14}O)_3PhO]_8PcCu$	6.39	291.5 (4.83)	339.5 (4.96)	615.5 (4.68)	652.0 (4.64)	684.0 (5.43)

(n=10, 12 and 14).

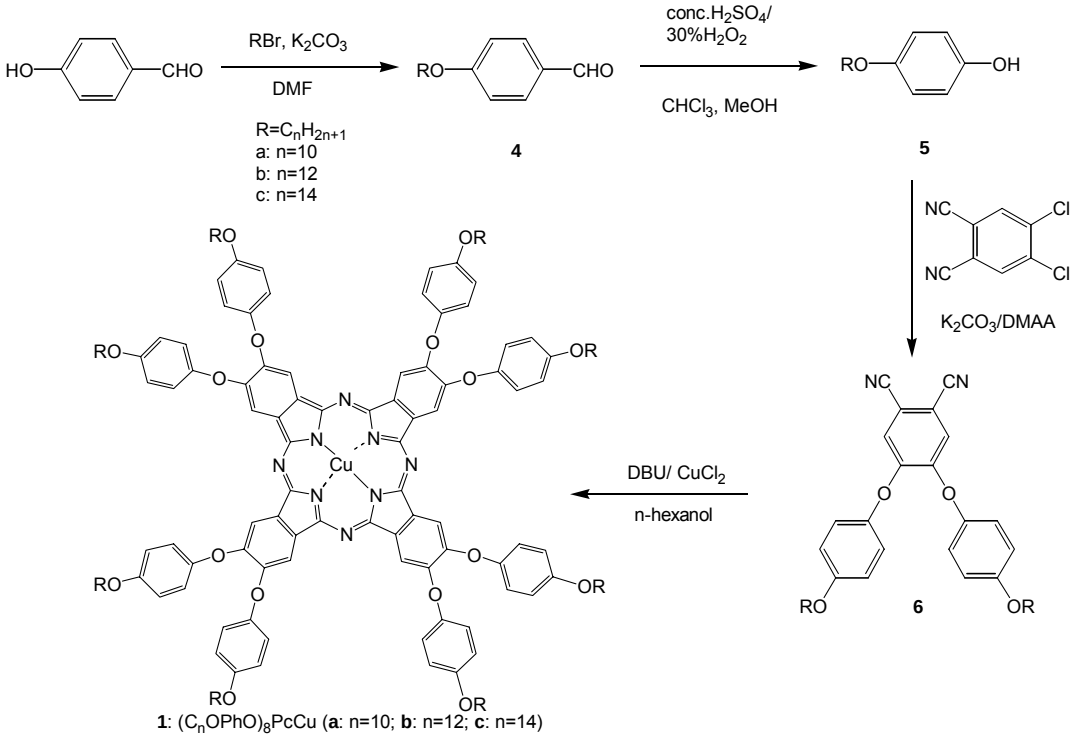
HO
CHO
RBr, K2CO3
DMF
R=CnH2n+1
a: n=10
b: n=12
c: n=14
RO
CHO
4
conc.H2SO4/
30%H2O2
CHCl3, MeOH
RO
OH
5
NC
Cl
NC
Cl
K2CO3/DMAA
NC
CN
O
O
RO
OR
6
DBU/ CuCl2
n-hexanol
RO
OR
O
N
Cu
1: (CnOPhO)8PcCu (a: n=10; b: n=12; c: n=14)

Scheme 1.

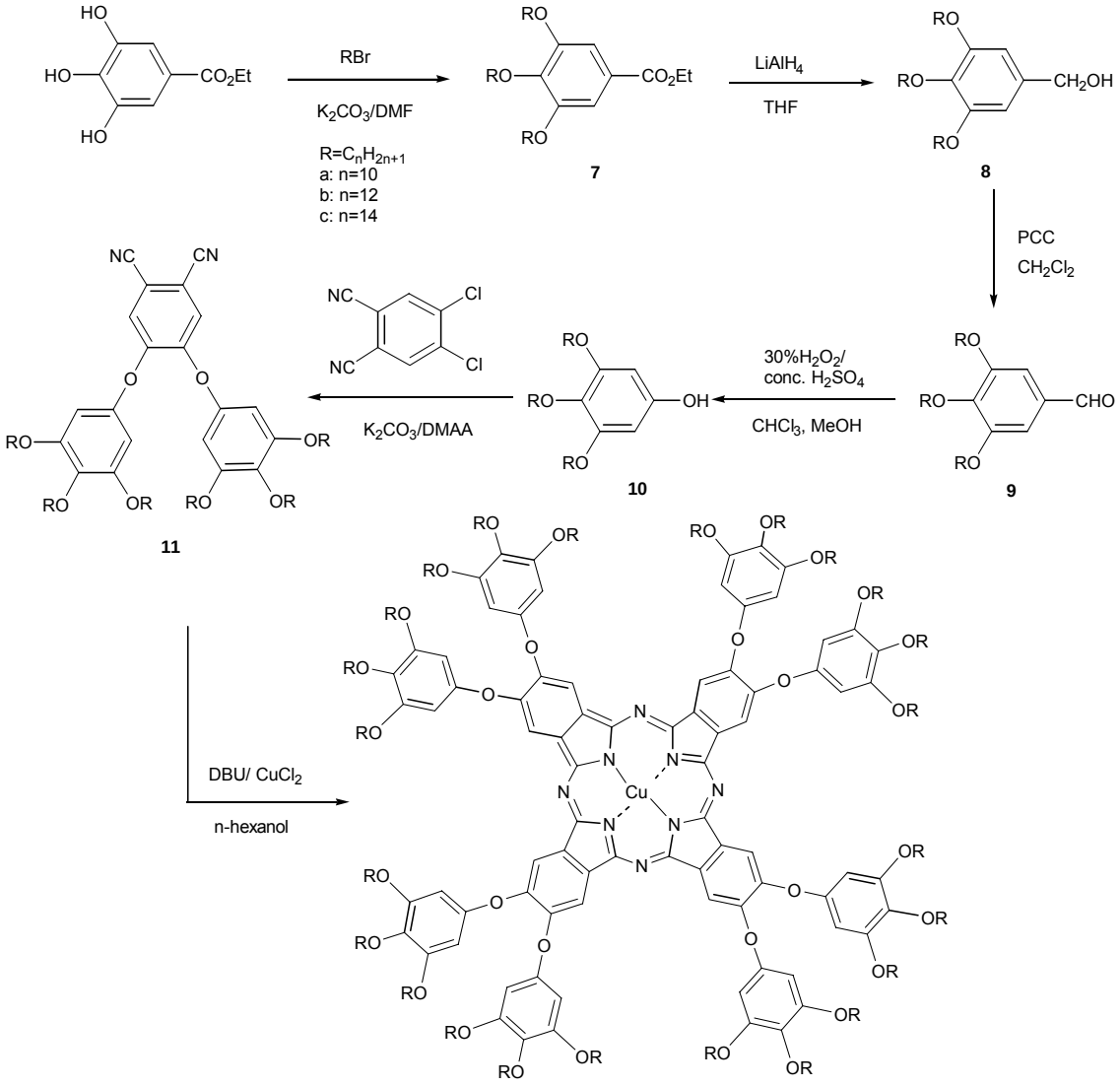

3: $[(C_nO)_3PhO]_8PcCu$ (**a**: n=10; **b**: n=12; **c**: n=14)

Scheme 2.

Table 3. Phase transition temperatures and enthalpy changes of $(C_nOPhO)_8PcCu$: **1**, $[(C_nO)_2PhO]_8PcCu$: **2** and $[(C_nO)_3PhO]_8PcCu$: **3** (n=10, 12 and 14).

Compound	Phase T/ °C [ΔH/ kJ mol^{-1}] Phase[a)]
1: $(C_nOPhO)_8PcCu$	
a: n=10	Cr_1 118.8 C_{r2} 122.6 Col_h [79.9][b)] 362.2 [7.94] I.L. (decomp.)
b: n=12	K 116.2 [98.7] Col_h 338.3 [19.2] I.L. ca. 350 decomp.
c: n=14	Cr_1 88.0 [4.62] Cr_2 113.9 [111.2] Col_h 292.3 [5.47] I.L. ca. 350 decomp.
2: $[(C_nO)_2PhO]_8PcCu$*	
a: n=10	Col_{hv} 104.4 [16.3] Col_{r1} ($P2_1/a$) 131.2 [7.61] Col_{r2} ($P2_1/a$) 142.4 [55.8] Col_{r3} ($P2_1/a$) 202.1 [4.11] I.L.; X_1 42.6 [3.20] X_2 80.4 [14.4]
b: n=12	X_v ca. 30-70 Col_h 106.0 [22.4] Col_{r1} ($P2_1/a$) 132.1 [65.0] Col_{r2} ($P2_1/a$) 149.2 Col_{tet} slow Cub ($Pn\bar{3}m$) 195.3 [3.54] I.L.; 176.0; 187.5 I.L.
c: n=14	X_v ca. 20-90 Col_h 111.2 [16.1] Col_r ($P2_1/a$) 125.6 [62.1] Col_{tet} slow Cub ($Pn\bar{3}m$) 180.9 [3.44] I.L.; 169.5; 175.5 I.L.
3: $[(C_nO)_3PhO]_8PcCu$	
a: n=10	X_v 37.6 [11.9] Col_r (P2m) 71.2 [6.95] Y 81.2 [8.11] Cub ($Pn\bar{3}m$) 176.9 [10.5] I.L.
b: n=12	X_v 27.6 [8.31] Col_r (P2m) 56.0 [7.12] Y 75.1 [1.16] Cub ($Pn\bar{3}m$) 159.6 [8.88] I.L.
c: n=14	Cr 36.8 Col_r (P2m) 45.9 [275][b)] Y 59.6 [2.26] Cub ($Pn\bar{3}m$) 144.8 [4.88] I.L.

a) Phase nomenclature: X=unidentified mesophase, Y=unidentified mesopahse Cr=crystal, Col_r=rectangular columnar mesophase, Col_h=hexagonal columnar mesophase, Col_{tet}=tetragonal columnar mesophase, Cub=bicontinuous cubic phase and I.L.=isotropic liquid. b) total enthalpy changes of the non-split peaks. v=Fresh virgin state obtained by recrystallization. *=prevous work by Hastusaka et al. See Ref.19.

(a)

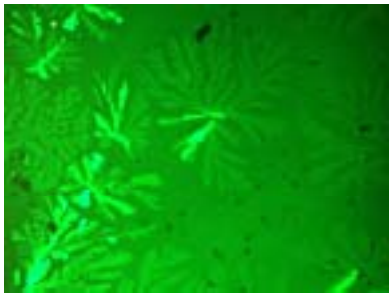

(b)

(c)

(d)

Figure 3.

Table 4. X-ray data of $(C_nOPhO)_8PcCu$: **1** (n = 10, 12 and 14) and $[(C_nO)_3PhO]_8PcCu$: **3** (n = 10, 12 and 14)..

Compound	Mesophase lattice constants/ Å	Spacing/ Å Observed	Calculated	Miller indices (h k l)
1a: $(C_{10}OPhO)_8PcCu$	Col_h at 200 °C	29.8	29.8	(1 0 0)
	a = 34.4	17.1	17.2	(1 1 0)
		14.8	14.9	(2 0 0)
		11.3	11.3	(2 1 0)
		ca. 4.6	-	#
1b: $(C_{12}OPhO)_8PcCu$	Col_h at 280 °C	30.4	30.4	(1 0 0)
	a = 35.1	17.9	17.6	(1 1 0)
		15.3	15.2	(2 0 0)
		11.7	11.5	(2 1 0)
		ca. 4.6	-	#
1c: $(C_{14}OPhO)_8PcCu$	Col_h at 260 °C	32.0	32.0	(1 0 0)
	a = 36.9	18.6	18.5	(1 1 0)
		16.1	16.0	(2 0 0)
		12.3	12.4	(2 1 0)
		ca. 4.7	-	#
3a: $[(C_{10}O)_3PhO]_8PcCu$	Col_r(P2m) at 65 °C	31.5	31.5	(1 1 0)
	a = 52.9	26.4	26.4	(2 0 0)
	b = 39.3	18.5	18.4	(1 2 0)
	h = 4.0*	16.1	16.1	(3 1 0)
	Z = *ca.* 1 for ρ = 1.00¶	11.7	11.7	(2 3 0)
		10.9	10.9	(4 2 0)
		8.90	8.81	(6 0 0)
		ca. 4.5	-	#
	Cub($Pn\bar{3}m$) at 155 °C	36.9	37.0	(2 1 1)
	a = 90.1	32.4	32.1	(2 2 0)
	Z = 89 for ρ = 1.00¶	29.6	30.2	(2 2 1)
		26.4	26.2	(2 2 2)
		24.4	24.3	(3 2 1)
		ca. 4.5	-	#
3b: $[(C_{12}O)_3PhO]_8PcCu$	Col_r(P2m) at 30 °C	34.0	34.0	(1 1 0)
	a = 60.9	30.4	30.4	(2 0 0)
	b = 40.9	24.5	24.4	(1 2 0)
	h = 4.0*	8.60	8.50	(3 1 0)
	Z = *ca.* 1 for ρ = 1.00¶	*ca.* 4.5	-	#
	Cub($Pn\bar{3}m$) at 135 °C	40.1	40.0	(2 1 1)
	a = 97.6	34.2	34.5	(2 2 0)
	Z = 97 for ρ = 1.00¶	32.0	32.5	(2 2 1)
		28.7	28.3	(2 2 2)
		26.3	26.2	(3 2 1)
		ca. 4.4	-	#
3c: $[(C_{14}O)_3PhO]_8PcCu$	Col_r(P2m) at 40 °C	37.4	37.4	(1 1 0)
	a = 66.3	33.2	33.2	(2 0 0)
	b = 45.3	19.0	18.7	(2 2 0)
	h = 4.0*	16.8	16.6	(4 0 0)
	Z = *ca.* 1 for ρ = 1.00¶	10.6	10.7	(2 4 0)
		9.70	9.50	(7 0 0)
		9.12	9.11	(0 5 0)
		8.50	8.61	(5 4 0)
		ca. 4.5	-	#
	Cub($Pn\bar{3}m$) at 124 °C	39.4	39.8	(2 2 0)
	a = 97.6	32.5	32.5	(2 2 1)
	Z = 87 for ρ = 1.00¶	29.2	29.4	(2 2 2)
		26.6	26.2	(3 2 1)
		14.7	14.7	(6 2 2)
		ca. 4.4	-	#

#: Halo of molten alkoxy chains. * : Assumed stacking distance. ¶: Assumed density (g/cm^3).

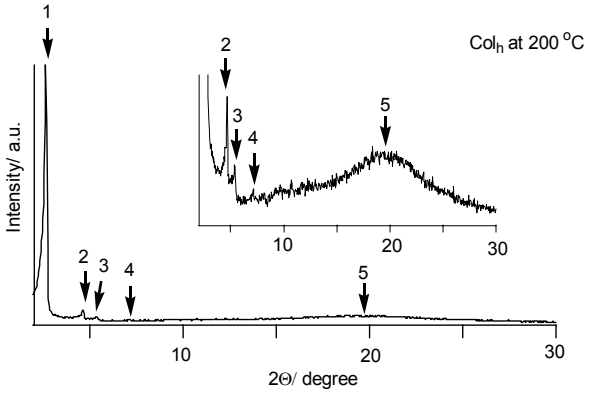

Figure 4.

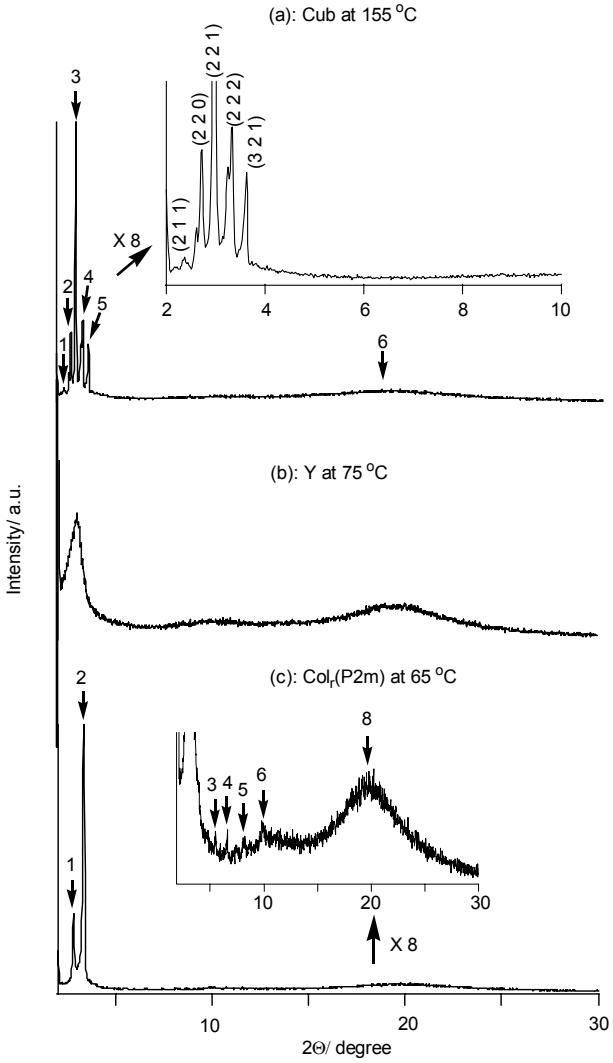
(a): Cub at 155 °C
3
(2 2 1)
(2 2 0)
(2 2 2)
(3 2 1)
(2 1 1)
X 8
2
4
5
1
6
2 4 6 8 10
(b): Y at 75 °C
Intensity/ a.u.
(c): Col$_r$(P2m) at 65 °C
2
8
3 4 5 6
1
10 20 30
X 8
10 20 30
2Θ/ degree

Figure 5.

Table 5. Extinction rules for the space group of bicontinuous cubic phases.

$h^2 + k^2 + l^2$	(h k l)	Pn3m (224)	Im3m (229)	Ia3d (230)
1	1 0 0	×	×	×
2	1 1 0	○	○	×
3	1 1 1	○	×	×
4	2 0 0	○	○	×
5	2 1 0	×	×	×
6	2 1 1	○	○	○
8	2 2 0	○	○	○
9	3 0 0	×	×	×
	2 2 1		×	×
10	3 1 0	○	○	×
11	3 1 1	○	×	×
12	2 2 2	○	○	○
13	3 2 0	×	×	×
14	3 2 1	○	○	○
16	4 0 0	○	○	○

○: appear. ×: disappear.

Table 6. X-ray data of $[(C_nO)_2PhO]_8PcCu$: **2** (n = 12 and 14)..

Compound	Mesophase lattice constants/ Å	Spacing/ Å Observed	Calculated	Miller indices (h k l)
2b: $[(C_{12}O)_2PhO]_8PcCu$	Cub($Pn\bar{3}m$) at 192 °C	40.5	40.6	(2 1 1)
	a = 99.5	35.6	35.2	(2 2 0)
	Z = 139 for ρ = 1.00¶	32.7	33.1	(2 2 1)
		30.4	30.0	(3 1 0)
		29.4	28.8	(3 1 1)
		27.1	27.4	(3 2 1)
		ca. 4.4	-	#
3c: $[(C_{14}O)_2PhO]_8PcCu$	Cub($Pn\bar{3}m$) at 179°C	37.1	37.5	(2 2 1)
	a = 112.7	35.6	35.6	(3 1 0)
	Z = 183r ρ = 1.00¶	34.2	34.0	(3 1 1)
		32.2	32.5	(2 2 2)
		30.7	30.2	(3 2 1)
		28.1	28.2	(4 0 0)
		ca. 4.4	-	#

#: Halo of molten alkoxy chains. * : Assumed stacking distance. ¶: Assumed density (g/cm^3).

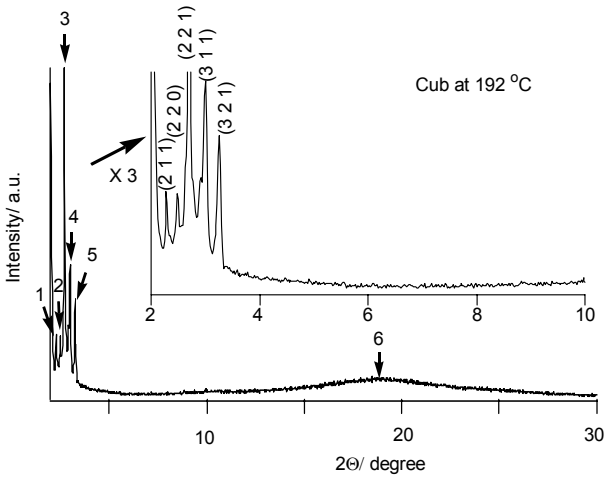
3
(2 2 1)
(3 1 1)
Cub at 192 °C
(3 2 1)
(2 2 0)
X 3
(2 1 1)
4
5
1
2
Intensity/ a.u.
2
4
6
8
10
6
10
20
30
2Θ/ degree

Figure 6.

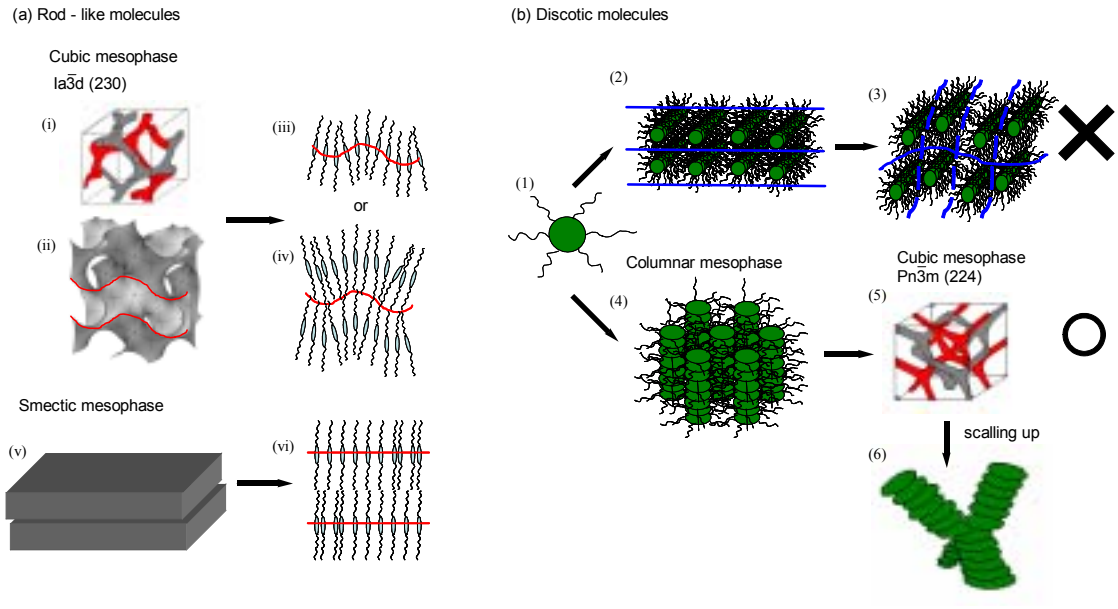
(a) Rod - like molecules
Cubic mesophase
Ia3̄d (230)
(i)
(ii)
(iii)
or
(iv)
Smectic mesophase
(v)
(vi)
(b) Discotic molecules
(1)
(2)
(3)
(4)
Columnar mesophase
Cubic mesophase
Pn3̄m (224)
(5)
scalling up
(6)

Figure 7.